RNA (1999), *5*:1200–1209. Cambridge University Press. Printed in the USA.

mRNA localization signals can enhance the intracellular effectiveness of hammerhead ribozymes

NAN SOOK LEE,[1] EDOUARD BERTRAND,[2] and JOHN ROSSI[1,3]

[1]Department of Molecular Biology, Beckman Research Institute of the City of Hope, Duarte, California 91010-3011, USA
[2]J. Monod, Tour 43, 2 Place Jussieu, 75251 Paris, France
[3]Graduate School of Biological Sciences, City of Hope and Beckman Research Institute of the City of Hope, Duarte, California 91010-3011, USA

ABSTRACT

Subcellular localization signals for several mRNAs are positioned in their 3′ untranslated regions (UTR). We have utilized the human α- and β-actin 3′ UTRs as signals for colocalizing hammerhead ribozymes with a *lacZ* target mRNA. Ribozyme and target genes containing matched or unmatched 3′ UTRs were cotransfected into 12-day-old chicken embryonic myoblast and fibroblast (CEMF) cultures and assayed by *in situ* hybridization (ISH) using a dual label, antibody sandwich procedure, and dual fluorescence microscopy to monitor intracellular colocalization. β-galactosidase localization in transfectants was visualized by incubation with X-gal and also quantitated by an *o*-nitrophenyl β-*D*-galactopyranoside (ONPG) assay. We found that the percentage of colocalization using the matched α- or β-actin 3′ UTR (α–α or β–β) was enhanced approximately threefold relative to unmatched 3′ UTRs. The increase in ribozyme-mediated inhibition of β-galactosidase activity observed when matched 3′ UTRs were used was consistent with the observed percentage of colocalization. These results represent the first direct demonstration that mRNA localization signals (zipcodes) can be utilized to enhance intracellular ribozyme efficacy.

Keywords: 3′ UTR; colocalization; hammerhead ribozyme; human α-actins; human β-actins

INTRODUCTION

The discovery that certain RNA species possess catalytic activity has generated significant interest in the potential therapeutic use of catalytic RNA molecules (ribozymes) in controlling gene expression (for a review, see Christoffersen & Marr, 1995). Ribozymes have been shown to function *in trans* and can be directed against foreign target sequences by flanking the catalytic core with sequences complementary to the target (Uhlenbeck, 1987; Haseloff & Gerlach, 1988). The hammerhead is the smallest of the known ribozyme motifs and therefore amenable to experimental manipulation (for a review, see Symons, 1992). Hammerhead ribozymes have broad potential as therapeutic agents for the selective control of gene expression (for a review, see Haseloff & Gerlach, 1988; Sarver et al., 1990; Christoffersen & Marr, 1995). An important problem confronting the use of hammerhead ribozymes as therapeutic agents is that of maximizing the interaction of ribozymes to their target RNAs in vivo. Experiments employing the unique property of retroviruses to dimerize prior to and during packaging have provided a paradigm for ribozyme–target colocalization (Sullenger & Cech, 1993; Pal et al., 1998). The dimerization and packaging of retroviral RNAs creates a unique physical association of two genomic RNAs. When a ribozyme is tethered to the dimerization domain, the physical interaction of two dimerization sequences facilitates the base pairing of ribozyme to target. Physical associations of nonviral RNAs occur within cells, but these usually involve specific base pairing interactions such as snRNAs with splicing signals (Wu & Manley, 1991; Sun & Manley, 1995; Incorvaia & Padgett, 1998). The interaction of U1 snRNA with the 5′ splice signal has been used as an approach for colocalization of a ribozyme with an HIV target (Michienzi et al., 1998).

More subtle methods for ribozyme–target colocalization can take advantage of the properties of some messenger RNAs to be localized within specific subcellular compartments. The first evidence for cytoplasmic mRNA localization came from the observation that actin tran-

Reprint requests to: John Rossi, Department of Molecular Biology, Beckman Research Institute of the City of Hope, Duarte, California 91010-3011, USA; e-mail: jrossi@coh.org.

scripts are unevenly distributed in ascidian embryos (Jeffery et al., 1983). Subsequently, several maternal mRNAs were identified in *Xenopus* (Melton, 1987) and *Drosophila* (Frigerio et al., 1986) that are localized during oogenesis, and many mRNAs are localized in neurons (Garner et al., 1988; Burgin et al., 1990; Tiedge et al., 1991) and oligodendrocytes (Ainger et al., 1993). Localized mRNAs have also been discovered in somatic cells (Hill & Gunning, 1993; Kislauskis et al., 1993). In chicken embryonic fibroblasts and myoblasts, β-actin mRNA is localized to the leading lamellae at the cell periphery, whereas α-actin transcripts are associated with the perinuclear compartment (surrounding the nucleus) (Kislauskis et al., 1993). RNA localization has also been reported in the yeast, *Saccharomyces cerevisiae*, and functions during budding (Long et al., 1997; Takizawa et al., 1997).

The ability of actin mRNAs to be transported and anchored in particular subregions of the cytoplasm involves *cis*-acting elements found in the mRNAs (Sundell & Singer, 1991). *Cis*-acting localization signals have been identified in a number of mRNAs, and many lie within the 3′ UTR (Jackson, 1993; Wilhelm & Vale, 1993; Decker & Parker, 1995; Bashirullah et al., 1998). The localization signal ("zipcode" within the 3′ UTR was sufficient to localize heterologous reporter molecules to the appropriate compartments in the cytoplasm of chicken embryonic myoblasts and fibroblasts (CEMFs) (Kislauskis et al., 1993, 1994). These studies demonstrated that the first 54 nt of the human β-actin 3′ UTR localized *lacZ* mRNA in chicken cells in a manner quantitatively indistinguishable from the homologous segment of the chicken β-actin 3′ UTR.

Capitalizing on the localization properties of RNAs could facilitate intracellular functioning of ribozymes by allowing them to colocalize with their target mRNA. To test this hypothesis, we utilized the 3′ UTR-encoded localization signals of the human α- and β-actins to colocalize a hammerhead ribozyme with its *lacZ* mRNA target. We demonstrate that ribozyme and substrate RNAs containing matched 3′ UTRs have statistically significant increases in colocalization in comparison to constructs containing unmatched 3′ UTRs. This colocalization occurs in 20% of the CEMF cells using either human α- or β-actin 3′ UTR. We also observe a decrease in β-galactosidase activity consistent with the observed extent of ribozyme–target colocalization using the matched human actin 3′ UTRs (α–α or β–β).

RESULTS

In vitro ribozyme cleavage

The constructs used in this study are shown in Figure 1 and described in Materials and Methods. To verify ribozyme cleavage, radiolabeled substrate *lacZ* mRNA (378 nt) was incubated with varying amounts of in vitro-transcribed ribozyme for 1 h (Fig. 2). Cleavage efficiency increased with increasing concentration of ribozyme (Fig. 2, lanes 3–8). No cleavage products were observed with the mutant ribozymes (Fig. 2, lanes 1 and 2) or ribozymes incubated in the absence of Mg^{2+} (Fig. 2, lane 9).

Colocalization of substrate and ribozyme

To determine whether the 3′ UTRs of human actin mRNA could direct colocalization of ribozyme and substrate transcripts to the same subcellular compartments, pRSV-βgal and pHook-GFP Rbz constructs fused to the α- or β-actin 3′ UTRs were cotransfected into CEMFs and analyzed as described in Materials and Methods.

We first determined the distribution of β-galactosidase activity and green fluorescent protein (GFP). These techniques allowed us to visualize indirectly the subcellular localization of ribozyme and substrate mRNAs via their translational products (Kislauskis et al., 1993). Following a period of transient expression, intracellular β-galactosidase activity was detected in single CEMF cells by a brief incubation with X-gal. GFP expression was visualized using a fluorescence microscope. The human α-actin 3′ UTR directs localization to a perinuclear array whereas the human β-actin 3′ UTR directs localization to the peripheral cytoplasm as visualized by X-gal staining for β-galactosidase activity (Fig. 3A,B). GFP expression was also preferentially concentrated in a perinuclear array using the α-actin 3′ UTR, whereas it was concentrated in the peripheral cytoplasm using the β-actin 3′ UTR (Fig. 3C,D). β-galactosidase activity or GFP expression, however, was also observed outside of these subcellular locations. To confirm that the matched 3′ UTRs can colocalize the substrate and ribozyme, the human β-actin 3′ UTR appended to ribozyme and target transcripts was tested first because peripheral cytoplasmic localized expression can be readily distinguished from nonlocalized expression. Both *lacZ* and ribozyme transcripts localized to the peripheral cytoplasm in cells (about 5%, $n = 100$) (Fig. 3E,F). However, we also observed colocalization in nonperipheral cytoplasmic areas of the cell (about 20%, $n = 100$) (data not shown). β-galactosidase or GFP expression from mRNAs lacking specific localization signals appeared in the cytoplasm as homogeneously distributed X-gal staining or fluorescence (data not presented).

In situ hybridizations using RNA probes were performed to determine directly the subcellular localization of substrate and/or ribozyme RNAs. pRSV-βgal and pHook-GFP Rbz fused with the human α- and β-actin 3′ UTRs were cotransfected into CEMFs. RNA probes complementary to either the substrate or ribozyme were hybridized to the transcripts *in situ*, and hybrids were detected by antibody staining as shown in Figure 4. From these data it can be seen that the ribozyme–

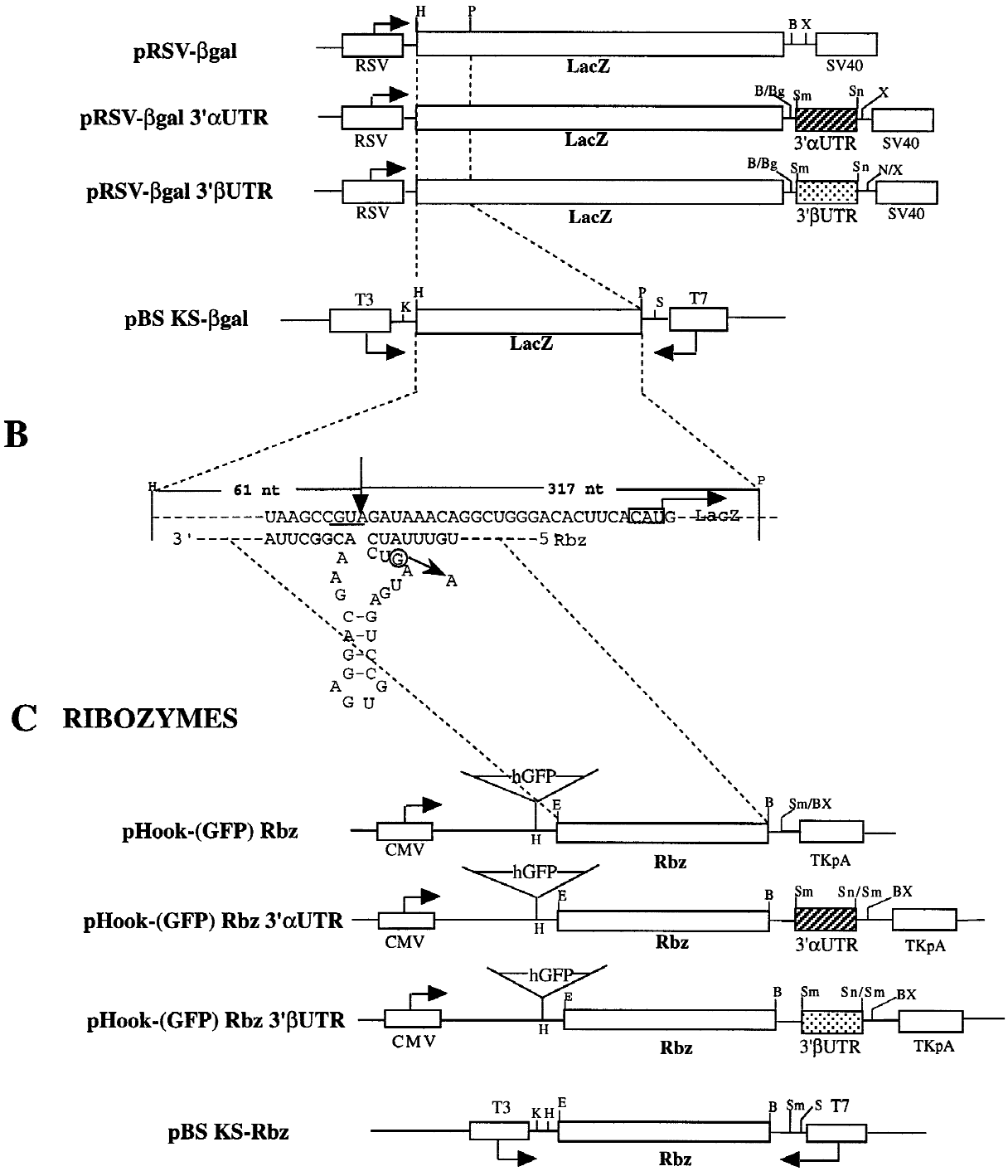

FIGURE 1. Constructs used for testing ribozyme–target colocalization employing the human α- and β-actin 3′ UTRs. **A**,**C**: The respective 3′ UTRs were appended to the *lacZ* reporter construct, which is under transcriptional control of the RSV promoter (**A**) and anti-*lacZ* ribozyme under transcriptional control of the CMV promoter (**C**). The ribozyme cassettes are incorporated in the pHook-2 vector. For in vitro transcription of the ribozymes and substrates for the ribozyme cleavage reactions and *in situ* hybridization of RNA, the ribozyme and target sequences are also cloned into pBluescript KS. **B**: The anti-*lacZ* ribozyme hybridized to the target site in the *lacZ* mRNA. The ribozyme is designed to cleave 3′ of the underlined GUA. Replacement of G5 (circled) by A produces a catalytically inactive ribozyme variant. Following the *in vitro* ribozyme cleavage reactions, the sizes of the cleavage products are 61 and 317 nt. B: *Bam*HI; Bg: *Bgl*II; BX: *Bst*XI; E: *Eco*RI; H: *Hin*dIII; hGFP: humanized green fluorescent protein; K: *Kpn*I; P: *Pvu*II; N: *Nhe*I; S: *Sac*I; Sm: *Sma*I; Sn: *Sna*BI; SV40: SV40 polyadenylation signal; T3: T3 promoter; T7: T7 promoter; TKpA: thymidylate kinase polyadenylation signal; X: *Xba*I.

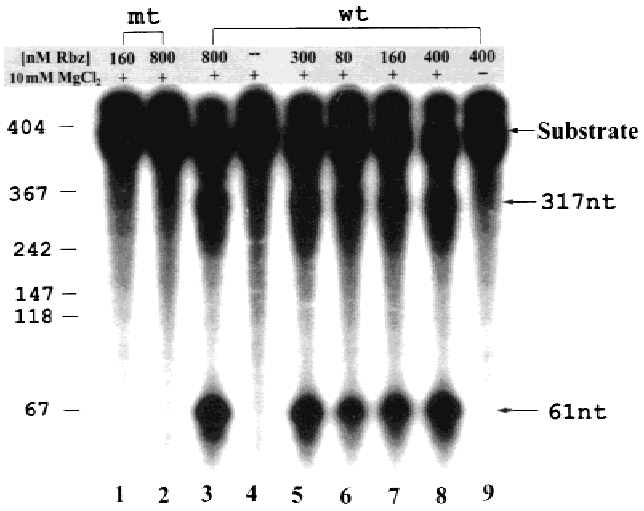

FIGURE 2. Ribozyme-mediated in vitro cleavage of *lacZ* mRNA. Radiolabeled substrates (8 nM) were incubated with ribozymes for 1 h at 37 °C. Lanes 3–8 show cleavage reactions as a consequence of increasing ribozyme concentrations. The position of cleavage products is indicated at 317 nt and 61 nt. No cleavage of radiolabeled substrate *lacZ* mRNA is seen in the absence of ribozyme (lane 4) or Mg^{2+} (lane 9), or following incubation with the mutant ribozyme (lanes 1 and 2). The left panel shows migration of DNA molecular weight markers.

α-actin 3′ UTR transcripts preferentially localize to the perinuclear region (Fig. 4A, green, FITC) and the substrate containing the same 3′ UTR also preferentially localizes to this region (Fig. 4A, red, CY3). A dual filter was used to detect overlapping signals (Fig. 4A, yellow). It should be noted that the overlapping signals (yellow) in the perinuclear region were observed in less than 5% of the cells, but approximately 20% of the cells showed overlapping signals in other cytoplasmic regions (data not shown). Therefore, we scored all cells with overlapping signals using low-power magnification. Statistical analyses of the percentage of transfectants showing overlap indicated that the matched 3′ UTR sequences significantly increased the frequency of colocalization of the ribozyme and its target (significance from Student's *t* test was $P < 0.01$, see Fig. 5). In cells containing matched α-actin 3′ UTRs (α–α), the percentage of colocalization was increased 3.4-fold relative to unmatched 3′ UTRs (α–β) (24.7% versus 7.2%; Fig. 5A). We conclude from these data that colocalization of the ribozyme and substrate is improved with matched α-actin 3′ UTRs, but discrete perinuclear localization only accounted for a small percentage of this.

The β-actin 3′ UTR directs localization to a peripheral region of CEMFs (Kislauskis et al., 1993; Fig. 4B). Signal overlap in the peripheral region of CEMFs was observed in $<$5% of the cells. In 20% of the cells, overlap was found in regions other than the peripheral cytoplasm of the CEMFs (data not shown). Matched β-actin 3′ UTRs (β–β) increased the percentage of colocalization by 3.1-fold relative to the nonhomologous 3′ UTRs (β–α) (20.6% versus 6.7%; Fig. 5B).

These data indicate that ribozymes and substrates containing matched 3′ UTRs show an approximate threefold increase in colocalization compared to constructs containing unmatched 3′ UTRs, and colocalization occurs in about 20% of the transfected CEMF cells using either the human α- or β-actin 3′ UTRs.

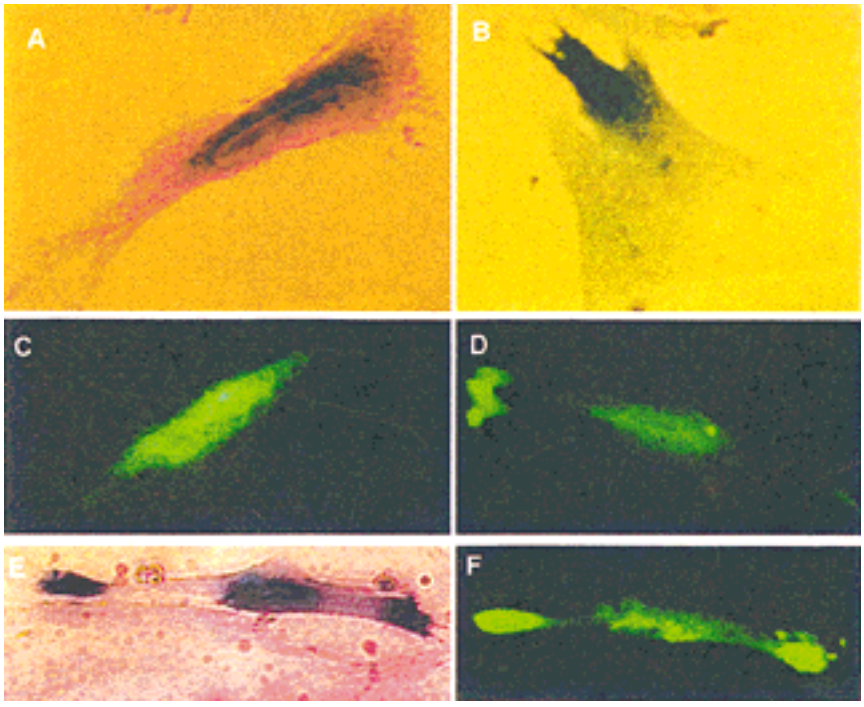

FIGURE 3. Subcellular localization of substrate and ribozymes in CEMFs as a function of the human actin 3′ UTR zipcodes. **A**,**B**: Visualization of β-galactosidase activity following transient transfection of pRSV-βgal appended with human actin 3′ UTRs. The human α-actin 3′ UTR zipcode localizes β-galactosidase in a perinuclear array (**A**) whereas the β-actin 3′ UTR zipcode specifies localization to the peripheral cytoplasm (**B**). **C**,**D**: Localization of GFP-human actin 3′ UTR chimeras as a marker for ribozyme expression in magnetically selected, transiently transfected cells. The human α-actin 3′ UTR localized GFP expression in a perinuclear array (**C**), and the human β-actin 3′ UTR in the peripheral cytoplasm (**D**). **E**,**F**: Colocalization of β-galactosidase activity and GFP expression when both are appended with the β-actin 3′ UTR. β-galactosidase (**E**) and GFP (**F**) activities can be visualized in the peripheral cytoplasm as well as in the central cytoplasm, indicating colocalization of substrates and ribozyme.

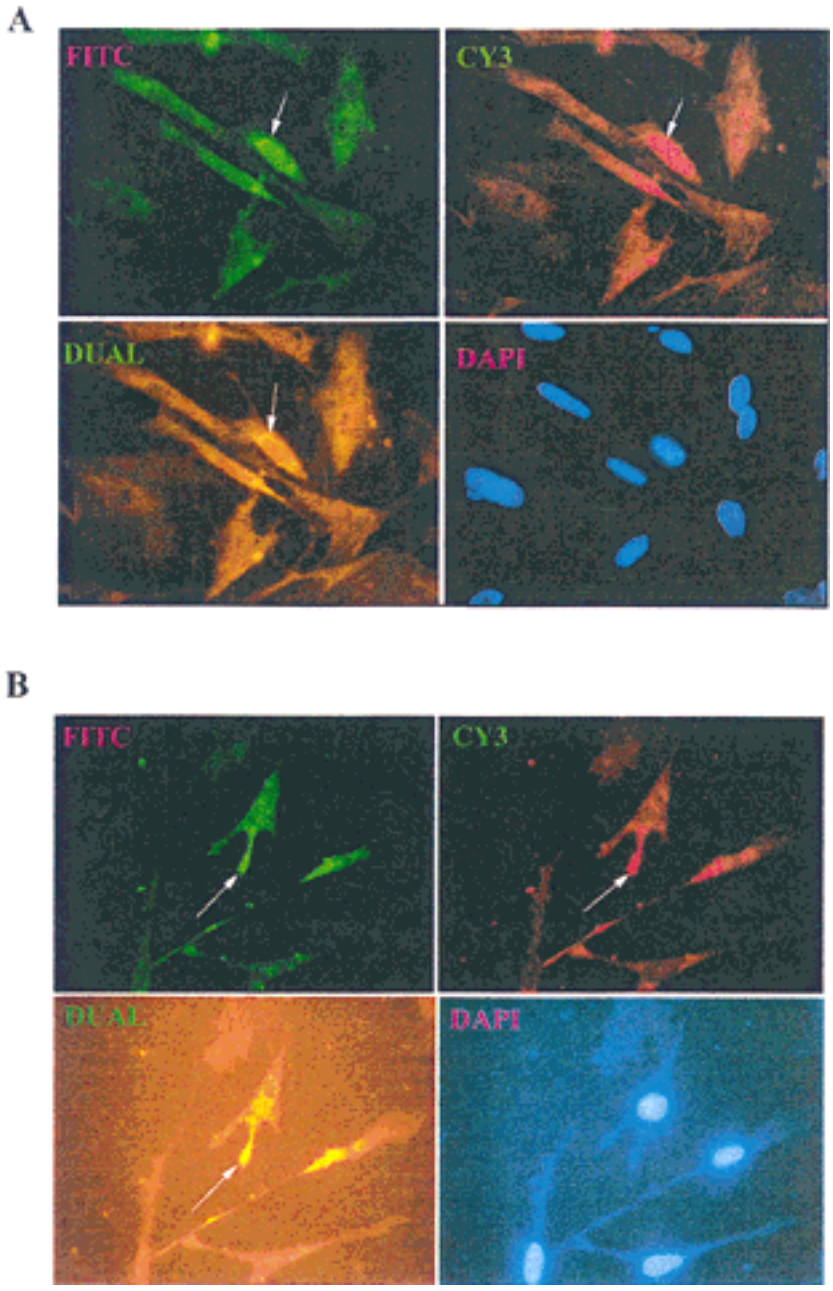

FIGURE 4. Colocalization of the target and ribozyme RNAs as a function of appended 3′ UTRs. pRSV-βgal (target) and pHook-GFP Rbz (ribozyme) constructs with the indicated appended actin 3′ UTRs cotransfected into CEMFs. Magnetic selection was carried out to enrich for transfected cells. *In situ* hybridization using RNA probes was performed on the magnetically selected CEMFs, which were recultured on gelatin-coated coverslips. The distribution of *in situ* reaction products was examined by fluorescence microscopy at 600× magnification. Detection of the ribozyme and RNAs was accomplished using FITC (top left) and Cy3 (top right) filters, respectively. The appended 3′ UTRs are α-actin (**A**) and β-actin (**B**). A dual filter (FITC+Cy3) (bottom left) was used to detect overlapping ribozyme and target signals. Nuclear identification was accomplished through DAPI staining (bottom right).

Intracellular ribozyme function

Given the threefold increase in colocalization with matched 3′ UTRs, we examined whether this corresponded to enhanced ribozyme function in transfected cells. To investigate this possibility, we assayed β-galactosidase activity after magnetically selecting cells cotransfected with pHook-ribozymes and substrates containing matched (α–α or β–β) and unmatched (α–β, α–No, or β–α, β–No) 3′ UTRs (see Materials and Methods). Results of the β-galactosidase activity measurements are shown in Figure 6. β-galactosidase activity measurements in cells cotransfected with substrate and pHook vector alone (without cloned ribozyme genes) were used as controls. Statistical analyses of the relative percent of β-galactosidase activity versus controls indicated that the most significant reduction in β-galactosidase activity was achieved when the ribozyme and *lacZ* target RNAs were colocalized with matched 3′ UTRs (Fig. 6A,B). Colocalization using the α-actin 3′ UTRs (α–α) resulted in an additional 30–36% reduction of β-galactosidase activity relative to the noncolocalized (α–β, α–No) mRNAs (Fig. 6A). A crippled, mutant ribozyme control with matched 3′ UTRs (α–α) resulted in about 68% of the level of reduction of β-galactosidase activity obtained with the functional ri-

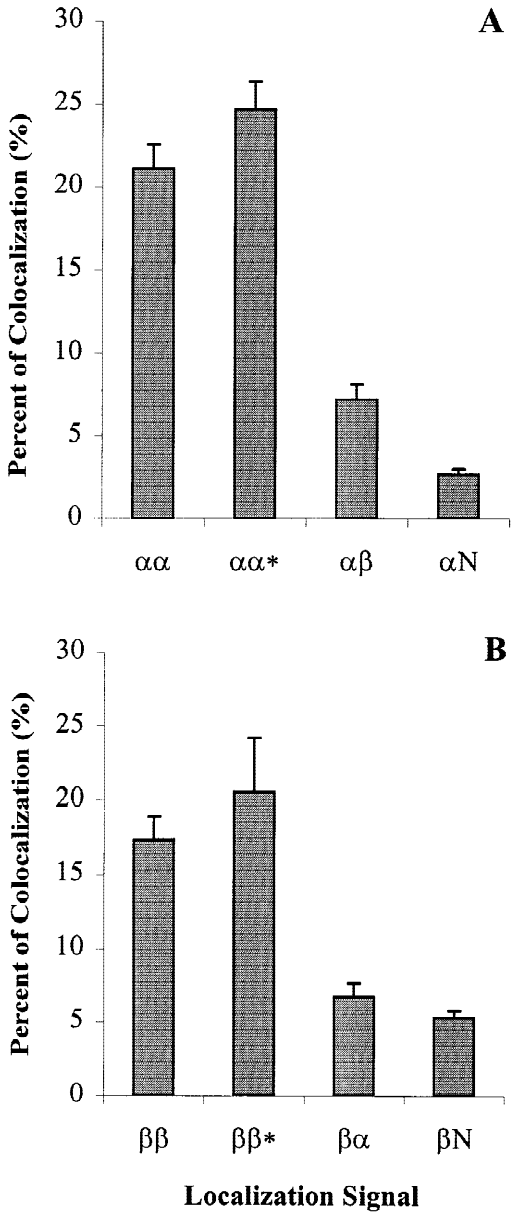

FIGURE 5. Effects of α- (**A**) and β- (**B**) actin 3′ UTR sequences on the colocalization of substrate and ribozyme. pRSV-βgal (target) and GFP-ribozyme constructs fused with either the α-actin (1:1 ratio of target and ribozyme) or β-actin (1:5 ratio of target and ribozyme) 3′ UTR were cotransfected into CEMF cells. Ribozyme construct transfectants were magnetically selected and subjected to *in situ* hybridization with ribozyme and target specific probes. To evaluate the percentage of cells with colocalized transcripts, the *in situ* reaction products were examined under low magnification using the dual FITC and Cy3 filter (yellow). Data is expressed as the percent of colocalized transfectant number (yellow color) relative to the total cell number measured by DAPI staining. In the figure, the first letter depicts the source of 3′ UTR for the target, and the second letter depicts the source of the 3′ UTR for the ribozyme. The asterisks indicate that the ribozyme construct was the inactive mutant. The mutant ribozyme was used as a control for potential loss of colocalization signal as a consequence of ribozyme mediated cleavage and subsequent destruction of the target. No significant differences were observed in the colocalization ratios of the functional versus mutant ribozyme experiments. αN and βN depict transfections in which the target was cotransfected with parental pHook-2 vector lacking a ribozyme. The data represent three independent experiments for each construct. From each experiment, dual filter counting was repeated four to eight times to arrive at the mean and standard deviations (error bars).

bozyme using matched 3′ UTRs (α–α) (27% versus 40%).

Colocalization using the β-actin 3′ UTR resulted in a more dramatic enhancement of ribozyme function compared to noncolocalized RNAs (Fig. 6B). The relative β-galactosidase activity of the matched 3′ UTRs (β–β) was reduced by 42–57% compared to the unmatched localization signals (β–α or β–No). Moreover, the reduction of β-galactosidase activity by the mutant ribozyme with matched UTRs (β–β) was only 27% of that observed with the functional ribozyme (β–β; 18% versus 71%).

DISCUSSION

We have taken advantage of the localization function of the human α- and β-actin 3′ UTRs to test the functional consequences on ribozyme activity. We observed that both ribozyme and substrate harboring the same 3′ UTR signals (zipcodes) are delivered to the same subcellular compartments, but this localization is not complete. Based on our data, the matched 3′ UTRs (α–α or β–β) allowed the anti-*lacZ* ribozyme to colocalize with the *lacZ* substrate RNAs about threefold more efficiently than when unmatched 3′ UTRs (α–β or β–α) were used. Colocalization occurred in approximately 20% of the cells using either the human α- or β-actin 3′ UTR. Although this number is statistically significant ($P < 0.01$), this is less than the specific subcellular localization of *lacZ* message observed when only a single RNA species was being tracked (43.4% and 31.2% for α- and β-3′ UTR-containing messages, respectively), and considerably less than the peripheral localization of the endogenous β-actin (40–60%; Kislauskis et al., 1993). This discrepancy may in part be due to saturation of cellular factors required for localization when both ribozyme and target transcripts are coexpressed in the presence of the endogenous actin transcripts.

Analyses of the percent inhibition of β-galactosidase activity as a function of matched versus unmatched 3′ UTRs suggested that β-actin 3′ UTR-matched ribozyme and target resulted in the greatest amount of ribozyme-mediated inhibition. Under these conditions, there was a 2.5–3.2-fold enhancement of ribozyme inhibition using the matched versus the unmatched 3′ UTRs. Some reduction of β-galactosidase activity relative to vector controls was mediated by a mutant form of the ribozyme, although this reduction was in the same percentage range as that observed with nonlocalized controls and presumably reflects the antisense contribution in these assays.

In the case of the α-actin 3′ UTR, a slight but reproducible improvement in ribozyme function was associated with use of matched 3′ UTRs. This slight improvement with 3′ UTR-mediated colocalization suggests some enhancement in ribozyme–target inter-

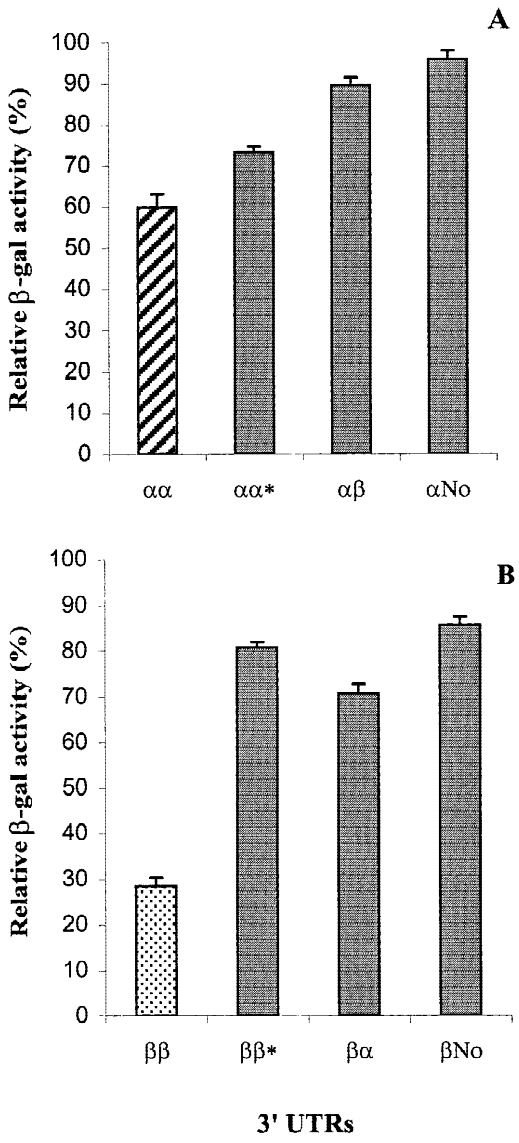

FIGURE 6. Effects of colocalization on intracellular ribozyme function. Constructs harboring the indicated combinations of appended 3′ UTRs were cotransfected into CEMFs. Transfectants were enriched by magnetic selection and cells were assayed for β-galactosidase activity using ONPG (Materials and Methods). Relative quantitation of β-galactosidase activity is based upon the values obtained with ribozyme and target cotransfection relative to the values obtained from the negative controls in which cells were cotransfected with target and empty (no ribozyme) pHook-2 vector. The β-galactosidase units obtained for the negative controls were 569, 195, and 70 U for α-actin, and 622, 268, and 74 U for β-actin for 1:1, 1:5, and 1:10 ratios of substrate to empty pHook-2 vector, respectively. The optimal ribozyme-to-substrate vector ratios for the α- and β-3′ UTR constructs were determined to be 1:1 and 10:1, respectively. These ratios were used for the experiments presented in this figure. The first letter indicates the source of 3′ UTR for the target and the second for the ribozyme. The asterisks indicate that the ribozyme construct was the inactive mutant. No indicates nonlocalizing 3′ UTR obtained from the herpes TK gene. Colocalized transfectants are depicted as hatched columns for α-actin 3′ UTRs (**A**) and dotted columns for β-actin 3′ UTRs (**B**), respectively. Each bar represents the average of three to nine independent experimental trials. RNase protection assays were also carried out on fibroblasts transfected with each of the ribozyme constructs. The results and quantitation of these assays demonstrated no significant differences in levels of ribozyme containing transcripts as a function of the appended 3′ UTR (data not shown).

actions as a consequence of colocalization, but not as significant as that observed with the βUTR signal. These results suggest that the mechanisms of mRNA localization may differ between the α- and β-actin 3′ UTRs. Alternatively, the perinuclear localization directed by the α-UTR may not provide a concentrated enough environment for ribozymes and substrate to effectively interact.

There are four mechanisms for mRNA localization identified so far: (1) spatial control of mRNA stability, (2) anchoring to localized binding sites, (3) vectorial nuclear export, and (4) directed transport (St Johnston, 1995). The α-actin 3′ UTR-coupled messages may diffuse from the perinuclear region to the cytoplasm without strong association with the cytoskeleton. Thus, the zipcode from the α-actin 3′ UTR does not direct the RNAs to a highly concentrated environment that can facilitate ribozyme–target interactions. In contrast, the β-actin 3′ UTR-mediated localization to the peripheral cytoplasm provides a more discrete and concentrated localization for such interactions. This is accomplished via active transport to the peripheral cytoplasm, followed by anchoring. Whatever the mechanisms for mRNA localization using the α- and β-actin 3′ UTRs in the CEMF cells, the localization signals from the α- and β-actin 3′ UTRs did not interfere with interaction between the ribozyme and the substrate (Fig. 6).

Ribozyme mediated destruction of targeted mRNAs in cells is dependent upon several factors. Given that the site chosen for cleavage is accessible to base pairing by the ribozyme, it can only pair if it comes in contact with the target RNA. Thus in vivo, the ribozyme–target association step is the most critical parameter for obtaining ribozyme function. Gross colocalization of ribozyme and target transcripts can be accomplished by trafficking to the same general compartment (nucleus versus cytoplasm) (Bertrand et al., 1997). This often results in only a slight enhancement of ribozyme function. Thus far the most effective strategies for enhancing intracellular ribozyme function have taken advantage of unique means for colocalizing ribozyme and message transcripts (Sullenger & Cech, 1993; Michienzi et al., 1998; Pal et al., 1998). Since some messenger RNAs have discrete intracellular subcompartmentalization that is encoded in the 3′ UTR, it is reasonable to take advantage of this property to colocalize ribozymes with their targets. We have demonstrated that in fact this form of colocalizations can be utilized to enhance ribozyme efficacy for messages that harbor specific intracellular localization signals.

3′ UTR-encoded localization signals found in localized messages of somatic cells may not be sufficiently strong to ensure complete compartmentalization of all messages containing such a signal. Subcellular localization of specific RNAs has also been reported in oocytes and during early embryonic development. In *Drosophila*, the maternal bicoid and oskar mRNAs are

localized to the anterior and posterior poles of the egg, respectively. The spatial organization of their encoded protein products is thought to be essential to establishing the basic body plan of the fly (Nusslein-Volhard et al., 1987; Driever & Nusslein-Volhard, 1988; Macdonald & Struhl, 1988; St Johnston et al., 1989; Ephrussi et al., 1991; Kim-Ha et al., 1991; Bashirullah et al., 1998; Berleth et al., 1998). In *Xenopus*, the Vg1 mRNA localized to the vegetal pole of the oocyte (Melton, 1987; Weeks & Melton, 1987). In *S. cerevisiae,* ASH1 mRNA is tightly localized within the budding daughter cell (Long et al., 1997; Takizawa et al., 1997). Each of these mRNAs has its localization signal in the 3′ UTR. These three localized messages are tightly confined to their subcellular sites during specific stages of development or during yeast budding, and may thus provide more stringent tests for colocalizing ribozymes with target mRNAs. The present studies provide the first direct test of utilizing mRNA localization signals for colocalization of ribozyme and target RNAs. We are presently exploring the potential advantages of the more complete and discrete localization of the oskar and Ash1 mRNAs to further test concept of 3′ UTR-mediated colocalization of ribozyme and target mRNAs to improve ribozyme efficacy.

MATERIALS AND METHODS

Substrate RNA constructs

All constructs were verified by restriction endonuclease analyses and dideoxy sequencing. The plasmid RSV βgal contains a *lacZ* reporter gene, a polylinker and an SV-40 3′ polyadenylation signal (Kislauskis et al., 1993). The pRSV-βgal was used for constructing substrate RNA plasmids containing the human α- or β-actin 3′ UTRs. The human α-actin 3′ UTR was generated from human genomic DNA by PCR (upper primer: 5′aactgc**agatct**tctagacccgggCTAAGATGCCTTCT CTCTCCATC; lower primer: 5′-gc**tctaga**attcgctagtcacgta ACAATGCTCAGGGTGTCAAAGCA). The restriction sites used for cloning are indicated by lowercase letters. The resultant *Bgl*II-*Xba*I (bold letters) restriction fragment generated by partial digestion was cloned into the *Bam*HI and *Xba*I sites of pRSV-βgal, yielding pRSV-βgal 3′ αUTR (Fig. 1A). The 3′ UTR of β-actin was also derived by PCR from human genomic DNA [*Bgl*II-*Nhe*I (bold letters) restriction fragment] (upper primer: 5′-aactgc**agatct**ctagacccgggTAGGCGGAC TATGACTTAGTTGC: lower primer: 5′-aagcttgaattc**gcta gc**tacgtaccCACCCTCTGCTGCCCCCAACCA) (pRSV-βgal 3′ βUTR, Fig. 1A). For in vitro transcriptions, 378-nt *Hin*dIII-*Pvu*II restriction fragments from the plasmids were cloned into pBluescript™ KS(+), yielding pBS KS-βgal.

Ribozyme constructs

The hammerhead ribozyme motif used in this study contains eight nucleotide-binding arms complementary to the *lac*Z message (Fig. 1B). In the inactive ribozyme variants, the critical G5 was an A, which renders the ribozyme inactive. *Eco*RI-*Bam*HI restriction fragments containing the ribozyme sequences were prepared from synthetic oligonucleotides (upper primer: 5′-cg**gaattc**cgTGTTTATCCTGATGAGTCCGTGAG GAC; lower primer: 5′-cg**ggatcc**cgcccgggTAAGCCGTT TCGTCCTCACGG) and by PCR amplification using overlapping (underlined) synthetic oligonucleotides (Rossi et al., 1982). They were cloned into *Eco*RI-*Bam*HI restriction sites of pBluescript™ KS+, yielding pBS KS-Rbz (Fig. 1C). This vector was used for in vitro transcription. For transfection experiments, the *lacZ Hin*dIII-*Sma*I restriction fragments of each RSV βgal 3′ UTR (Fig. 1A) were replaced by the ribozyme containing *Hin*dIII-*Sma*I restriction fragments from pBS KS-Rbz, yielding pRSV-Rbz 3′ α- or βUTR (not shown). The *Hin*dIII-*Sna*BI fragments containing both the ribozyme and each of the 3′ UTRs were cleaved from each pRSV-Rbz 3′ α- or βUTR and inserted back into the *Hin*dIII-*Sma*I site of pHook2 (Invitrogen) (pHook-Rbz 3′ α- or βUTR, Fig. 1C). A 3′ αUTR *Sma*I-*Bst*XI fragment from pHook-Rbz 3′ αUTR was removed, filled in, and relegated to yield pHook-Rbz (Fig. 1C). To enzymatically follow the localization of the ribozymes, the humanized green fluorescent protein (hGFP) 730-nt *Not*I fragment from pTR-UF (Zolotukhin et al., 1996) was filled in and subcloned into the *Hin*dIII-cut and filled-in site of pHook-Rbz 3′ UTR yielding pHook-GFP Rbz or pHook-GFP Rbz 3′ α- or βUTR (Fig. 1C).

RNA synthesis and in vitro cleavage reactions

In vitro transcripts were prepared according to the supplier (MEGAscript™; Ambion). The ribozymes were transcribed with T3 RNA polymerase using pBS KS-Rbz linearized with *Bam*HI. Transcripts were purified by phenol/chloroform extraction and ethanol precipitation, and dissolved in 50 mM Tris-HCl, pH 7.5, 1 mM EDTA at a final concentration of 50 ng/μL. Radiolabeled substrates were transcribed with T3 RNA polymerase from pBS KS-βgal linearized with *Pvu*II in the presence of [α-^{32}P]UTP (Amersham). After a 2-h incubation at 37 °C, the RNAs were treated with RNase-free DNase I (Boehringer Mannheim), followed by gel purification. RNA concentrations were determined spectrophotometrically. Cleavage reactions were performed as previously described (Bertrand et al., 1994). Ribozymes and substrates were heated separately for 1 min at 90 °C in water, incubated 5 min at room temperature in cleavage buffer (20 mM Tris-HCl, pH 7.5, 10 mM $MgCl_2$, 150 mM NaCl), mixed, and then incubated at 37 °C. Reactions were stopped by addition of 40 mM EDTA, and analyzed by electrophoresis in denaturing polyacrylamide gels and autoradiography.

Transfection

Twelve-day-old chicken embryonic myoblasts and fibroblasts were grown in DMEM supplemented with 10% fetal calf serum, 2 mM L-glutamine and 10 mL/L Fungi-Bact solution. Transfections were performed with the calcium phosphate coprecipitation procedure according to the supplier (Gibco BRL). Cells were plated at a density of 1×10^6 cells/100 mm plate in 10 mL complete medium. After 24 h, and 3 h prior to transfection, cells were fed with fresh complete medium. Cells were then mixed with 20 μg coprecipitates of plasmid DNA containing different ratios of substrate and ribozyme (1:1, 1:5,

and 1:10) followed by incubation for 10–24 h, at which time old medium was removed and replaced with fresh medium. After 24 h, a magnetic selection for pHook-2 transfectants (containing the ribozyme genes) was carried out according to instructions provided by the supplier (Invitrogen). pHook-2 can express and display a single-chain antibody (sFv) against a specific hapten on the surface of transfected cells. Cells expressing the sFv can then be isolated from the culture by binding to hapten-coated magnetic beads (Invitrogen). For *in situ* hybridization, the selected transfectants were plated onto 0.5% gelatin-coated coverslips. The next day cells were fixed in 4% formaldehyde and 10% glacial acetic acid in PBS for 10 min and washed twice with PBS. The cells were permeablized with 70% ethanol overnight at 4 °C.

RNA probes

pBS KS-βgal and pBS KS-Rbz were linearized with *Hin*dIII and *Eco*RI, respectively, for T7 polymerase-directed antisense RNA synthesis. RNAs were labeled by incorporating either digoxigenin- or biotin-conjugated UTP according to the manufacturer's description (Boehringer Mannheim Biochem.). To 1 μg of linearized template was added 1 μL of a 10 mM nucleotide mix (including 6.5 mM labeled UTP and 3.5 mM unlabeled UTP), 1 μL of 10$\times$ transcription buffer, 2 μL of T7 polymerase, 1 μL of RNase inhibitor, and water to a final volume of 10 μL. When the probes were more than 250 nt in length, mild alkaline hydrolysis was performed to generate smaller fragments of around 250 nt. The labeled probes were quantified spectrophotometrically.

In situ hybridization (ISH)

In situ hybridization was performed using in vitro transcribed digoxigenin- or biotin-labeled probes to detect ribozyme or substrate RNAs respectively. All chemicals were of RNA grade. Cells were prehybridized with 2$\times$ SSC and 50% formamide for 5 min at room temperature. Hybridization solutions were made fresh each time and contained 40 μg of denatured *Escherichia coli* tRNA and 24–50 ng of labeled probe in 20 μL formamide. This solution was incubated for 1 min at 85 °C and added to 20 μL of 2$\times$ hybridization solution (4$\times$ SSC, 20% dextran sulfate, 0.02% BSA, 2 mM vanadyl ribonucleoside complex). The prehybridization solution was removed and 40 μL of fresh hybridization solution was added to each coverslip and incubated at 37 °C overnight in a humidified container. For double hybridizations, both probes were added simultaneously. Slides were washed twice in 0.1$\times$ SSC and 50% formamide for 30 min at 50 °C. For antibody staining, all reactions were performed for 30 min at 37 °C in 40 μL of antibody buffer (AB; 3$\times$ SSC and 10% formamide) with 0.1% BSA and 2 mM vanadyl complex. After each reaction, the slides were washed twice with AB for 15 min at room temperature. For detecting ribozyme localization, a 1/200 dilution of sheep anti-digoxigenin antibody (Boehringer Mannheim), followed by a 1/150 dilution of donkey anti-sheep antibody conjugated with FITC (Sigma) were utilized. For detecting substrate, a 1/2,000 dilution of extravidin (Sigma), a 1/2,000 dilution of mouse anti-avidin conjugated with biotin (Sigma), and a 1/2,000 dilution of extravidin conjugated with Cy3 (Sigma) were used for the first, second, and third reactions, respectively. The slides were treated with antifading solution containing DAPI (Oncor).

Microscope image analysis

Digital image processing was used to analyze localization of ribozyme and substrate RNAs within cells. Images were collected using an Olympus BX50 microscope and a DEI-750 video camera (Optronics). A 60$\times$ objective and FITC and Cy3 filters were used to detect ribozyme and substrate signals, respectively. The dual filter for FITC + Cy3 was also used to simultaneously detect both signals that show as a yellow color, and the DAPI filter was used to identify the nucleus (blue). For counting overlapping signals within cells, at least four different images per set were obtained with a 10$\times$ objective and were stored using a dual filter for dual signals and a DAPI filter for total cell number. The automated count function of Image-Pro Plus (Media Cybernetics) was used to count the number of yellow and blue signals for dual labeled cells and nucleus, respectively. An obvious yellow signal was chosen to serve as a reference using color segmentation. The percent of colocalization is defined as the number of yellow cell images relative to the number of blue cell images (total cells) in the same field.

X-gal staining and GFP visualization

Cells were fixed in 1% glutaraldehyde, 0.1 M sodium phosphate buffer, pH 7.0, 1 mM $MgCl_2$, for 15 min at room temperature. The fixed cells were incubated in 0.2% X-gal solution (10 mM sodium phosphate buffer, pH 7.0, 120 mM NaCl, 1 mM $MgCl_2$, 3.3 mM ferro and ferri cyanide mix). After 30 min to 1 h, X-gal solution was removed and 70% glycerol was added. The blue-colored cells were identified under a phase-contrast light microscope (40$\times$ objective). GFP was used as a ribozyme expression marker in CEMF cells and visualized with a fluorescent microscope within 10 min following cotransfection. This short time was necessary to minimize diffusion of GFP protein from the site of translation.

In vivo β-galactosidase activity assay

After magnetic selection of transfected cells, β-galactosidase activities from CEMF transfectants were determined using *o*-nitrophenyl β-*D*-galactopyranoside (ONPG). Eight to ten million cells were collected, washed with PBS, and suspended in 150 μL suspension buffer (250 mM Tris-HCl, pH 7.6, 5 mM DTT). The resuspended cells were lysed three times by freezing and thawing in liquid nitrogen. After centrifugation, the supernatants were incubated with ONPG solution (0.8 mg/mL in Z buffer, pH 7.0, 60 mM $Na_2HPO_4 \cdot 7H_2O$, 40 mM $NaH_2PO_4 \cdot H_2O$, 10 mM KCl, 1 mM $MgSO_4 \cdot 7H_2O$, 50 mM β-mercaptoethanol) at 37 °C until a faint yellow color developed. Adding 0.5 mL of 1 M Na_2CO_3 stopped the reaction, and the length of time of incubation was recorded for each sample. The A_{420} was read against the control containing Z buffer alone. The total protein in the reaction mixture was calculated from the original sample concentration in milligrams per milliliter by Bio-Rad protein assay (Bio-Rad). The specific activity of the β-galactosidase is defined in units per

milligram as: $A_{420} \times 10^7/45 \times$ min at 37 °C $\times$ mg protein in reaction.

We observed the strongest effects of colocalization using a 1:1 ratio of ribozyme to target mRNA for the α-3′ UTR, and a 10:1 ratio for the β-3′ UTR. These ratios were used in the experiments reported in Fig. 6.

ACKNOWLEDGMENTS

We thank David Hessinger at Loma Linda University and Chauncey Bowers for providing the chicken embryos, Shawn Westaway for critical reading of this manuscript, and Paul Salvaterra for helpful discussions. This research was supported by National Institutes of Health grants AI9329 and AI42552.

Received February 5, 1999; returned for revision March 10, 1999; revised manuscript received June 17, 1999

REFERENCES

Ainger K, Avossa D, Morgan F, Hill SJ, Barry C, Barbarese E, Carson JH. 1993. Transport and localization of exogenous myelin basic protein mRNA microinjected into oligodendrocytes. *J Cell Biol 123*:431–441.

Bashirullah A, Cooperstock RL, Lipshitz HD. 1998. RNA localization in development. *Annu Rev Biochem 67*:334–394.

Berleth T, Burri M, Thoma G, Bopp D, Richstein S, Frigerio G, Noll M, Nusslein-Volhard C. 1998. The role of localization of bicoid RNA in organizing the anterior pattern of the Drosophila embryo. *EMBO J 7*:1749–1756.

Bertrand E, Castanotto D, Zhou C, Carbonnelle C, Lee NS, Good P, Chatterjee S, Grange T, Pictet R, Kohn D, Engelke D, Rossi JJ. 1997. The expression cassette determines the functional activity of ribozymes in mammalian cells by controlling their intracellular localization. *RNA 3*:74–88.

Bertrand E, Pictet R, Grange T. 1994. Can hammerhead ribozymes be efficient tools to inactivate gene function? *Nucleic Acids Res 22*:293–300.

Burgin KE, Waxham MN, Rickling S, Westgate SA, Mobley WC, Kelly PT. 1990. *In situ* hybridization histochemistry of Ca^{2+}/calmodulin-dependent protein kinase in developing rat brain. *J Neurosci 10*:1788–1798.

Christoffersen RE, Marr JJ. 1995. Ribozymes as human therapeutic agents. *J Med Chem 38*:2023–2037.

Decker CJ, Parker R. 1995. Diversity of cytoplasmic functions for the 3′ untranslated region of eukaryotic transcripts. *Curr Opin Cell Biol 7*:386–392.

Driever W, Nusslein-Volhard C. 1988. The bicoid protein determines position in the *Drosophila* embryo in a concentration-dependent manner. *Cell 54*:94–104.

Ephrussi A, Dickinson LK, Lehmann R. 1991. Oskar organizes the germ plasm and directs localization of the posterior determinant nanos. *Cell 66*:37–50.

Frigerio G, Burri M, Bopp D, Baumgartner S, Noll M. 1986. Structure of the segmentation gene paired and the *Drosophila* PRD gene set as part of a gene network. *Cell 47*:734–746.

Garner CC, Tucker RP, Matus A. 1988. Selective localization of messenger RNA for cytoskeletal protein MAP2 in dendrites. *Nature 336*:674–677.

Haseloff J, Gerlach WL. 1988. Simple RNA enzymes with new and highly specific endoribonuclease activities. *Nature 334*:584–591.

Hill MA, Gunning P. 1993. Beta and gamma actin mRNAs are differentially located within myoblasts. *J Cell Biol 122*:824–832.

Incorvaia R, Padgett RA. 1998. Base pairing with U6atac snRNA is required for 5′ splice site activation of U12-dependent introns in vivo. *RNA 4*:709–718.

Jackson RJ. 1993. Cytoplasmic regulation of mRNA function: The importance of the 3′ untranslated region. *Cell 74*:9–14.

Jeffery WR, Tomlinson CR, Brodeur RD. 1983. Localization of actin messenger RNA during early ascidian development. *Dev Biol 99*:408–417.

Kim-Ha J, Smith JL, Macdonald PM. 1991. oskar mRNA is localized to the posterior pole of the *Drosophila* oocyte. *Cell 66*:23–35.

Kislauskis EH, Li Z, Singer RH, Taneja KL. 1993. Isoform-specific 3′-untranslated sequences sort alpha-cardiac and beta-cytoplasmic actin messenger RNAs to different cytoplasmic compartments. *J Cell Biol 123*:164–172.

Kislauskis EH, Zhu X, Singer RH. 1994. Sequences responsible for intracellular localization of beta-actin messenger RNA also affect cell phenotype. *J Cell Biol 127*:441–451.

Long RM, Singer RH, Meng X, Gonzalez I, Nasmyth K, Jansen RP. 1997. Mating type switching in yeast controlled by asymmetric localization of ASH1 mRNA. *Science 277*:383–387.

Macdonald PM, Struhl G. 1988. *Cis*-acting sequences responsible for anterior localization of bicoid mRNA in *Drosophila* embryos. *Nature 336*:594–598.

Melton DA. 1987. Translocation of a localized maternal mRNA to the vegetal pole of *Xenopus* oocytes. *Nature 328*:80–82.

Michienzi A, Conti L, Varano B, Prislei S, Gessani S, Bozzoni I. 1998. Inhibition of human immunodeficiency virus type 1 replication by nuclear chimeric anti-HIV ribozymes in a human T lymphoblastoid cell line. *Hum Gene Ther 9*:621–628.

Nusslein-Volhard C, Frohnhofer HG, Lehmann R. 1987. Determination of anteroposterior polarity in *Drosophila*. *Science 238*:1674–1681.

Pal BK, Scherer L, Zelby L, Bertrand E, Rossi JJ. 1998. Monitoring retroviral RNA dimerization in vivo via hammerhead ribozyme cleavage. *J Virol 72*:8349–8353.

Rossi JJ, Kierzek R, Huang T, Walker PA, Itakura K. 1982. An alternate method for synthesis of double-stranded DNA segments. *J Biol Chem 257*:9226–9229.

Sarver N, Cantin EM, Chang PS, Zaia JA, Ladne PA, Stephens DA, Rossi JJ. 1990. Ribozymes as potential anti-HIV-1 therapeutic agents. *Science 247*:1222–1225.

St Johnston D. 1995. The intracellular localization of messenger RNAs. *Cell 81*:161–170.

St Johnston D, Driever W, Berleth T, Richstein S, Nusslein-Volhard C. 1989. Multiple steps in the localization of bicoid RNA to the anterior pole of the *Drosophila* oocyte. *Development 107*:13–19.

Sullenger BA, Cech TR. 1993. Tethering ribozymes to a retroviral packaging signal for destruction of viral RNA. *Science 262*:1566–1569.

Sun JS, Manley JL. 1995. A novel U2–U6 snRNA structure is necessary for mammalian mRNA splicing. *Genes & Dev 9*:843–854.

Sundell CL, Singer RH. 1991. Requirement of microfilaments in sorting of actin messenger RNA. *Science 253*:1274–1277.

Symons RH. 1992. Small catalytic RNAs. *Annu Rev Biochem 61*:641–671.

Takizawa PA, Sil A, Swedlow JR, Herskowitz I, Vale RD. 1997. Actin-dependent localization of an RNA encoding a cell-fate determinant in yeast. *Nature 389*:90–93.

Tiedge H, Fremeau RT Jr, Weinstock PH, Arancio O, Brosius J. 1991. Dendritic location of neural BC1 RNA. *Proc Natl Acad Sci USA 88*:2093–2097.

Uhlenbeck OC. 1987. A small catalytic oligoribonucleotide. *Nature 328*:596–600.

Weeks DL, Melton DA. 1987. A maternal mRNA localized to the vegetal hemisphere in *Xenopus* eggs codes for a growth factor related to TGF-beta. *Cell 51*:861–867.

Wilhelm JE, Vale RD. 1993. RNA on the move: The mRNA localization pathway. *J Cell Biol 123*:269–274.

Wu JA, Manley JL. 1991. Base pairing between U2 and U6 snRNAs is necessary for splicing of a mammalian pre-mRNA. *Nature 352*:818–821.

Zolotukhin S, Potter M, Hauswirth WW, Guy J, Muzyczka N. 1996. A "humanized" green fluorescent protein cDNA adapted for high-level expression in mammalian cells. *J Virol 70*:4646–4654.